Spectrum Coexistence of Satellite-borne Passive Radiometry and Terrestrial Next-G Networks

Mohammad Koosha and Nicholas Mastronarde
University at Buffalo, Department of Electrical Engineering
Email: {mkoosha, nmastron}@buffalo.edu

2024 IEEE International Conference on Communications Workshops (ICC Workshops) | 979-8-3503-0405-3/24/$31.00 ©2024 IEEE | DOI: 10.1109/ICCWORKSHOPS59551.2024.10615536

***Abstract*—Spectrum coexistence between terrestrial Next-G cellular networks and space-borne passive remote sensing (RS) is now gaining attention. One major question is how would this coexistence impact RS equipment? In this study, we develop a framework based on stochastic geometry to evaluate the statistical characteristics of radio frequency interference (RFI) affecting RS satellites. Specifically, we consider RFI originating from a large-scale terrestrial Next-G network that spans dense urban areas across the globe, where each urban area contains a cluster of cellular base stations (BSs) operating in the same frequency band as the RS satellite. For illustration, we assume that the network operates in the restricted L-band (1400-1427 MHz) with NASA's Soil Moisture Active Passive (SMAP) satellite. We use a Thomas Cluster Process (TCP) to model the distribution of terrestrial BSs and derive the RFI on SMAP's antenna's main- and side-lobes. We show that a large number of active clusters can operate in the restricted L-band without compromising SMAP's mission if they avoid interfering with the main-lobe of its antenna. This is possible thanks to SMAP's extremely low side-lobe antenna gains.**

***Index Terms*—Restricted L-band, Active-passive Spectrum Coexistence, SMAP, Interference Modeling, Large-Scale Terrestrial Cellular Networks, Stochastic Geometry, Soil Moisture.**

I. Introduction

The spectrum crunch has motivated extensive research on the coexistence of different wireless technologies within the same spectrum. One case that has been gaining attention in recent years involves the use of passive Radio Frequency (RF) bands, which are solely devoted to passive sensing applications such as remote sensing and radio astronomy, for active wireless communications. Specifically, the coexistence of terrestrial active wireless communications and Earth Exploration Satellite Service (EESS) systems is becoming a central topic of discussion [1]. A major question that needs to be answered is how and to what extent Radio Frequency Interference (RFI) would impact such EESS satellites?

While current research primarily examines spectrum sharing between terrestrial cellular networks and terrestrial passive sensing technologies [2], in this study, we develop a mathematical framework to model the RFI originating from a large-scale terrestrial cellular network and its impact on an EESS satellite. Specifically, we imagine clusters of cellular base stations (BSs) exposed to an EESS satellite, where each cluster has a number of BSs active in the same frequency band as the satellite. To account for the randomness of the position of the clusters on Earth and the number of active cells within a cluster, we use the Thomas Cluster Process (TCP) from stochastic geometry [3].

The work of M. Koosha and N. Mastronarde was supported in part by the NSF under Award #2030157.

For illustration, we develop our model based on the National Aeronautics and Space Administration (NASA) Soil Moisture Active Passive (SMAP) satellite [4], which is one of the latest RS satellites active in the restricted L-band ($1400 - 1427$ MHz). We assume that the network operates in Frequency Domain Duplexing (FDD) mode, such that the down-link channels (BSs) utilize the 27 MHz restricted L-band, while User Equipments (UEs) operate in out-of-band uplink channels. We develop the characteristic function of RFI from the BSs at both the main- and side-lobes of SMAP's antenna. Using the characteristic function, we then derive the average, variance, and higher central moments of the RFI. We also demonstrate that, due to the very low side-lobe gains of SMAP's antenna, a large number of terrestrial clusters can be active while exposed to SMAP's side-lobe without compromising the accuracy of SMAP's measurements.

The paper is organized as follows. In Section II we introduce SMAP's measurement mechanism, our methodology for RFI analysis, and other preliminaries. Section III is the main RFI analysis section. Section IV is the simulations and results section. Section V is the conclusion section.

II. Preliminaries

A. SMAP & Brightness Temperature

As depicted in Figure 1, SMAP has a 6-meter-wide conically-scanning golden mesh reflector with a 3-dB antenna beam-width of 2.4° that projects a footprint of roughly 40×40 km^2 with an Earth incident angle of 40° at an altitude of 685 km. An Ortho-Mode Transducer (OMT) feedhorn collects the reflected radiations from the mesh reflector and duplexes them separately into *vertical* and *horizontal* polarizations. Figure 2 shows a 2-dimensional cut of SMAP's antenna gain for the vertical polarization. Through sectorization, which is a common method in stochastic geometry, we represent SMAP's antenna gain for each polarization (p) as:

$$g = \begin{cases} g_{(ml)}, & \text{if } |d| \leq 1.2^\circ, \\ g_{(sl)}, & \text{if } |d| > 1.2^\circ, \end{cases} \tag{1}$$

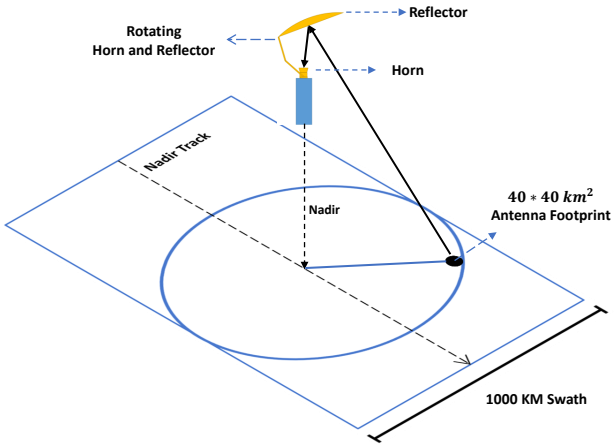

Figure 1: Horn and reflector rotation, beam footprint of the reflector, and SMAP's nadir track.

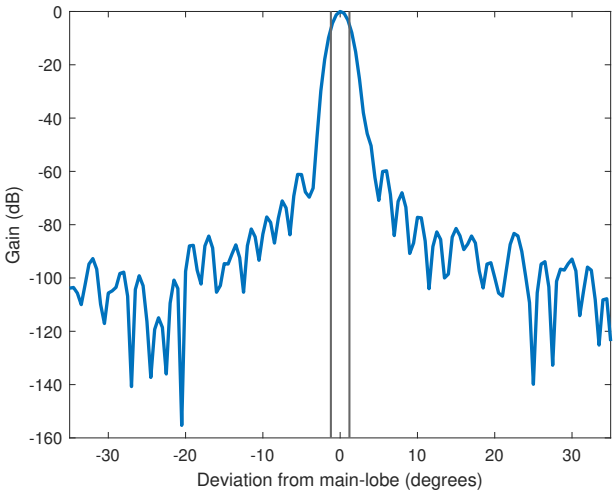

Figure 2: A 2-dimensional cut of SMAP's conical antenna gain for the vertical polarization. The gain for the horizontal polarization is similar. The two vertical lines show the 2.4° antenna beam-width.

where (ml) and (sl) stand for *main-lobe* and *side-lobe*, respectively, and $|d|$ is the deviation from the main-lobe axis. For each polarization (p), SMAP separately captures the *brightness temperature* of soil, $t_{soil}^{(p)}$ (in Kelvin), from the antenna footprint by capturing the soil's natural passive thermal radiations. These brightness temperature measurements can be translated to soil moisture content using models like the Tau-Omega mode [4]. We use the Nyquist noise formula [5] to convert electromagnetic power to brightness temperature as:

$$t^{(p)} = \frac{\mathrm{p}^{(p)}}{k_b \beta}, \tag{2}$$

where $\mathrm{p}^{(p)}$ is the electromagnetic power received by polarization (p), k_b is the *Boltzmann* constant, and β is the radio frequency *bandwidth*.

B. Methodology for RFI Analysis

In this section, we provide a concise explanation of the underlying logic guiding our analysis of RFI on SMAP. SMAP's measurements for each polarization can be seen as:

$$t_{meas} = t_{soil} + T_{RFI}, \tag{3}$$

where T_{RFI} denotes the RFI temperature at SMAP. Since T_{RFI} is a random variable, it causes uncertainty in SMAP's measurements. According to SMAP's documentation, uncertainties below threshold value $\tau = 1.3K$ are acceptable for SMAP's measurements [4]. To model T_{RFI} from a large terrestrial network, we imagine a set of $\{i\}$ Base Station (BS) clusters on the Earth-cut exposed to SMAP, where each cluster i comprises a set of $\{j\}_i$ BSs, each BS_{ij} has a (maximum) total electromagnetic transmission power p_{tx}, and P_{ij} is the amount of power received by SMAP from BS_{ij}. Clusters $\{i\}_{(ml)} \subset \{i\}$ are located on SMAP's main-lobe antenna footprint and clusters $\{i\}_{(sl)} \subset \{i\}$ are exposed to SMAP's side-lobe. Accordingly, T_{RFI} in (3), can be decomposed into its main- and side-lobe components as:

$$T_{RFI} = T_{(ml)} + T_{(sl)}, \tag{4}$$

where

$$T_{(l)} = \sum\nolimits_{\{i\}_{(l)}} \sum\nolimits_{\{j\}_i} T_{ij} \tag{5}$$

$$\text{with} \quad T_{ij} = \frac{P_{ij}}{k_b \beta} \tag{6}$$

where (l) is either (ml) or (sl). Assessing each P_{ij} would be a complicated function of BS_{ij} antenna angles, obstructions in the environment, and SMAP's elevation angle relative to BS_{ij}. However, based on Free Space Path Loss (FSPL), we note that:

$$P_{ij} \in \left[0,\ g\left(\frac{c}{4\pi f d_{ij}}\right)^{\alpha} p_{tx}\right] \tag{7}$$

and therefore, according to (6),

$$T_{ij} \in \left[0,\ g\eta\omega^{\alpha} d_{ij}^{-\alpha}\right], \tag{8}$$

where $\eta = \frac{p_{tx}}{k_b \beta}$, $\omega = \left(\frac{c}{4\pi f}\right)$, g is the gain of SMAP's antenna (based on (1), $g = g_{(ml)}$ if $i \in \{i\}_{(ml)}$, and $g = g_{(sl)}$ if $i \in \{i\}_{(sl)}$), c is the speed of light, f is the frequency, d_{ij} is the distance of BS_{ij} to SMAP, and $\alpha > 2$ is the path loss exponent. In (7), we ignore atmospheric loss since it is proven to have a negligible effect in the L-band [4]; however, this means that our model slightly overestimates the RFI.

We acknowledge that transient phenomena like fading and shadowing can cause temporary spikes in electromagnetic power. SMAP's documentation indicates a full-band integration time of 300 μs and a sub-band integration time of approximately 1.2 ms, emphasizing the need to address fast-fading effects. While fast-fading models could establish an upper limit for P_{ij} with confidence, we have opted to omit this in our current study for future research. Instead, for assessing maximum RFI on SMAP, we use $T_{ij} := g\eta\omega^{\alpha} d_{ij}^{-\alpha}$ in (5).

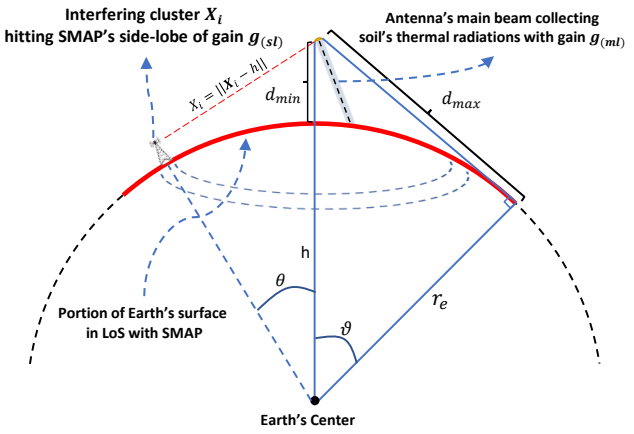

Figure 3: 2-dimensional representation of the Earth-cut exposed to the satellite. The red curve represents the maximum extent of the Earth-cut exposed.

This is akin to assuming the worst-case scenario, where all the transmission power from a single BS is directed solely towards the satellite.

C. Geometric Assumptions

As depicted in Figure 3, the Earth's center is the *origin* $(0,0,0)$ and SMAP is located at the point $\mathtt{h} = (0,0,h)$, where h is the distance of SMAP from the Earth's center. The area exposed to the satellite, shown with the red cap and encircled in $\theta \in [0, \vartheta]$ in Figure 3, is defined with the *Borel-set* $\mathcal{B} = \left\{ \|\mathtt{x}\| = r_e,\ \frac{\mathtt{x}\cdot\mathtt{h}}{\|\mathtt{x}\|\|\mathtt{h}\|} \geq \cos(\vartheta) \right\}$ in $\mathbb{R}^3$ measure space, where r_e is the Earth radius, $\|\cdot\|$ is the Euclidean norm, and $\cos(\vartheta) = \frac{r_e}{h}$. We define $\mathcal{B}_{(ml)} \subset \mathcal{B}$ as SMAP's antenna footprint projected on Earth and $\mathcal{B}_{(sl)} = \mathcal{B} \backslash \mathcal{B}_{(ml)}$ as the set of area exposed to the side-lobe of SMAP's antenna.

Let $\Psi = \{\mathbf{X}_i, i \in \mathbb{N}\} \subset \mathcal{B}$ denote a parent *Poisson Point Process* (PPP) with intensity measure $\Lambda(d\mathtt{x})$, where $\mathbf{X}_i$ denotes a cluster center. For simplicity we use a *homogeneous* PPP such that $\Lambda(d\mathtt{x}) = \lambda_c$. According to Figure 3, the minimum distance of a cluster center to SMAP is $d_{min} = h - r$, while the maximum distance is $d_{max} = \sqrt{h^2 - r_e^2}$. With $\psi = \{\mathtt{x}_i\}$ defined as a realization of Ψ, for each point $\mathtt{x} \in \psi$, we associate an *independent and identically distributed* (i.i.d) offspring PPP $\Xi_{\mathtt{x}}$. Each cluster $\Xi_{\mathtt{x}}$ consists of N i.i.d random points (BSs) where, according to a *Thomas Cluster Process* (TCP), $N \sim \mathsf{Pois}(\lambda_{BS})$. We define $\Phi \sim \mathcal{P}(\lambda_c, \lambda_{BS})$, where

$$\Phi = \bigcup\nolimits_{\mathbf{x}\in\Psi} (\mathbf{x} + \Xi_{\mathbf{x}}). \tag{9}$$

Accordingly, the cluster centers located in SMAP's main- and side-lobes are respectively $\Psi_{(ml)} = \Psi(\mathcal{B}_{(ml)})$ and $\Psi_{(sl)} = \Psi \backslash \Psi_{(ml)}$, and their respective clusters are $\Phi_{(ml)}$ and $\Phi_{(sl)}$.

Note 1. Defining $X_i = \|\mathbf{X}_i - \mathtt{h}\|$ as the distance of terrestrial cluster center $\mathbf{X_i}$ to SMAP and x_i as its realization, we assume that the cluster's dispersion $\ll x_i$, since an urban area is on the order of a few kilometers, while the cluster distance to SMAP is more than $d_{min} = 685$ km. Thus, for simplicity, we assume that the off-spring (BSs) within each cluster are equidistant (with distance x_i) to SMAP.

III. RFI Analysis

To assess the RFI brightness temperature T_{RFI} on SMAP as defined in (4), we analyze the statistical properties of RFI on SMAP's main- and side-lobes, i.e., its average, variance, and higher central moments, which help evaluating the skewness and kurtosis of T_{RFI}. For this purpose, we use the concepts of cumulants and Cumulant Generating Functions (CGFs).

Definition 1. The CGF of random variable X is defined as:

$$K(t) = \log \mathbb{E}[e^{tX}], \tag{10}$$

which is the log of the *Moment Generating Function* (MGF) $M(t) = \mathbb{E}[e^{tX}]$ of random variable X. Accordingly the nth *cumulant* of X is as follows:

$$k_n = K^n(0), \tag{11}$$

where $K^n(t)$ denotes the nth derivative of $K(t)$.

Remark 1. For random variable X, k_1 equals the first *raw* moment of X, i.e., $k_1 = \mathbb{E}[X]$. For $n \in \{2,3\}$, $k_n = \mu_n$, where $\mu_n = \mathbb{E}[(X - \mathbb{E}[X])^n]$ is the nth *central* moment of X. Consequently, the variance of X is its 2nd central moment, i.e., $k_2 = \mu_2$. Lastly, higher order central moments μ_n for $n > 3$ can be acquired by a combination of cumulants of X. For example, $\mu_4 = k_4 + 3(k_2)^2$.

Based on Definition 1 and Remark 1, we shift our focus on finding the MGF of $T_{(ml)}$ and $T_{(sl)}$ defined in (4). For this purpose, we start with the MGF of RFI brightness temperature of one cluster of BSs.

A. MGF for one Cluster

One key quantity that can help us determine the total RFI brightness temperature at SMAP is the maximum RFI brightness temperature contributed by *one* cluster. Assuming the cluster is located at point $\mathtt{x} \in \psi$ and comprises N BSs that are equidistant to SMAP, we have:

$$T_{cluster}(\mathtt{x}) = g\eta\omega^{\alpha}\|\mathtt{x} - \mathtt{h}\|^{-\alpha} N. \tag{12}$$

Corollary 1. *For a cluster located at point $\mathtt{x} \in \psi$ with $N \sim \mathsf{Pois}(\lambda_{BS})$ equidistant BSs (with distance $x = \|\mathtt{x} - \mathtt{h}\|$) to the satellite, the MGF of* (12) *is as follows:*

$$M_{cluster}(t;\ x,\ g) = \exp\left(\lambda_{BS}\left(-1 + \exp\left(g\eta\omega^{\alpha}x^{-\alpha}t\right)\right)\right). \tag{13}$$

Proof. Since N is a Poisson random variable, the MGF of N is $M_N(t) = \exp(\lambda_{BS}(e^t - 1))$. By setting $t := g\eta\omega^{\alpha}x^{-\alpha}t$, we acquire (13). □

$T_{\text{cluster}}(\mathtt{x})$ in (12) is the fundamental unit of RFI brightness temperature in our model. We obtain its series expansion to facilitate the calculation of RFI brightness temperature cumulants later on.

Lemma 1. *The series expansion of* (13) *is as follows:*

$$M_{cluster}(t;\ x,\ g) = \sum_{n=0}^{\infty} p_n(\lambda_{BS}) \left(g\eta\omega^{\alpha}x^{-\alpha}\right)^n \frac{t^n}{n!}, \quad (14)$$

with:

$$p_n(\lambda_{BS}) = \sum\nolimits_{i=0}^{n} S(n,i)\lambda_{BS}^i, \quad (15)$$

where $S(n,i)$ is the Stirling number of the second kind.

Proof. From [6], we know that:

$$\exp\left(v(e^t-1)\right) = \sum_{n=0}^{\infty} B_n(v)\frac{t^n}{n!}, \quad (16)$$

where $B_n(v)$ is the Bell polynomial of order n, and can be expanded as:

$$B_n(v) = \sum\nolimits_{i=0}^{n} S(n,i)v^i. \quad (17)$$

By setting $t := g\eta\omega^{\alpha}x^{-\alpha}t$ and $v = \lambda_{BS}$ in (16), we acquire (14). □

B. MGF on SMAP's Main- and Side-lobes

1) SMAP's main-lobe: The RFI brightness temperature $T_{(ml)}$ on SMAP's main-lobe is caused by all the clusters $\mathtt{x} \in \psi_{(ml)}$ in SMAP's main-lobe antenna footprint: i.e.,

$$T_{(ml)} = \sum\nolimits_{\mathbf{X}_i \in \Psi_{(ml)}} T_{cluster}(\mathbf{X}_i). \quad (18)$$

Note 2. Given that SMAP's antenna footprint is relatively small compared to the distance to the satellite, we assume a uniform distribution, envisioning that all cluster centers within the main-lobe antenna footprint ($\mathtt{x} \in \psi_{(ml)}$) are approximately equidistant from the satellite. Under this assumption, the distance to the satellite for the clusters in the main-lobe, $d_{(ml)}$, is the answer to the following quadratic equation:

$$d_{(ml)}^2 + 2d_{(ml)}r_e\sin(40^{\circ}) + r_e^2 - h^2 = 0 \quad (19)$$

Lemma 2. *With the assumption of $M \sim \mathsf{Pois}(\Lambda)$ equidistant $d_{(ml)}$ clusters from the satellite located in SMAP's main-lobe antenna footprint $\mathcal{B}_{(ml)}$, where $\Lambda = \lambda_c v^2(\mathcal{B}_{(ml)})$ and $v^2(\cdot)$ is a Lebesgue measure in $\mathbb{R}^2$, the MGF of $T_{(ml)}$ defined in* (18) *is as follows:*

$$M_{(ml)}(t) = \exp\left(40^2\lambda_c\left(-1 + M_{cluster}(t;\ d_{(ml)},\ g_{(ml)})\right)\right), \quad (20)$$

where $M_{cluster}(t;\ x,\ g)$ is defined in (13)*.*

Proof. Refer to Appendix A. □

2) SMAP's side-lobe: In this section, we investigate the maximum RFI brightness temperature $T_{(sl)}$ on SMAP's side-lobe defined in (4), which we can rewrite as:

$$T_{(sl)} = \sum\nolimits_{\mathbf{X}_i \in \Psi_{(sl)}} T_{cluster}(\mathbf{X}_i), \quad (21)$$

where $T_{cluster}(\mathbf{X}_i)$ is defined in (12).

Lemma 3. *The MGF of* (21) *is as:*

$$M_{(sl)}(t) = \exp\left(-2\pi\left(\frac{r_e}{h}\right)\lambda_c\int_{d_{min}}^{d_{max}}\left(1 - M_{cluster}(t;\ x,\ g_{(sl)})\right)x\,dx\right) \quad (22)$$

where $M_{cluster}(t;\ x,\ g)$ is defined in (13)*, and $d_{min} = h - r_e$ and $d_{max} = \sqrt{h^2 - r_e^2}$.*

Proof. Refer to Appendix B. □

C. Cumulants of RFI Brightness Temperature on SMAP's Main- and Side- Lobes

Now that we have the MGFs of $T_{(ml)}$ and $T_{(sl)}$, we are able to acquire their cumulants.

Lemma 4. *The nth cumulant of RFI brightness temperature $T_{(ml)}$ on SMAP's main-lobe, defined in* (18)*, is as follows:*

$$k_n^{(ml)} = 40^2 g_{(ml)}^n \eta^n \omega^{n\alpha}\lambda_c p_n(\lambda_{BS}) d_{(ml)}^{-n\alpha}, \quad (23)$$

where $p_n(\lambda_{BS})$ is defined in (15)*.*

Proof. The cumulants of $T_{(ml)}$ can be acquired using its MGF as defined in (20) and Definition 1. □

Corollary 2. *The expected value of $T_{(ml)}$ defined in* (18) *is:*

$$\mathbb{E}[T_{(ml)}] = 40^2 g_{(ml)}\eta\omega^{\alpha}\lambda_c\lambda_{BS}d_{(ml)}^{-\alpha}. \quad (24)$$

Proof. Based on Remark 1, the expected value of $T_{(ml)}$ is its first cumulant defined in (23). □

Corollary 3. *The variance of $T_{(ml)}$ defined in* (18) *is as:*

$$Var[T_{(ml)}] = 40^2 g_{(ml)}^2 \eta^2\omega^{2\alpha}\lambda_c(\lambda_{BS}^2 + \lambda_{BS})d_{(ml)}^{-2\alpha}. \quad (25)$$

Proof. Based on Remark 1, the variance of $T_{(ml)}$ is its second cumulant defined in (23). □

Lemma 5. *The nth cumulants of the RFI brightness temperature $T_{(sl)}$ on SMAP's side-lobe, defined in* (21)*, is as follows:*

$$k_n^{(sl)} = \frac{2\pi}{2-n\alpha}\left(\frac{r_e}{h}\right)g_{(sl)}^n\eta^n\omega^{n\alpha}\lambda_c p_n(\lambda_{BS})\left(d_{max}^{2-n\alpha} - d_{min}^{2-n\alpha}\right), \quad (26)$$

where $p_n(\lambda_{BS})$ is defined in (15)*.*

Proof. The cumulants of $T_{(sl)}$ can be acquired using its MGF as defined in (22) and Definition 1. □

Corollary 4. *The expected value of $T_{(sl)}$ defined in* (21) *is:*

$$\mathbb{E}[T_{(sl)}] = \frac{2\pi}{2-\alpha}\left(\frac{r_e}{h}\right)g_{(sl)}\eta\omega^{\alpha}\lambda_c\lambda_{BS}\left(d_{max}^{2-\alpha} - d_{min}^{2-\alpha}\right). \quad (27)$$

Proof. Based on remark 1, the expected value of $T_{(sl)}$ is its first cumulant defined in (26). □

Table I: SIMULATION PARAMETERS

Element	Value
Intensity of clusters (λ_C)	1 cluster (dense urban area) every 10000 km^2
Intensity of active BSs (λ_{BS})	50, 100, 200 BSs per cluster
Path loss exponent (α)	(2 , 2.2]
BS transmission power (p_{tx})	20 Watts per BS
Boltzmann's constant (k_b)	1.380649×10^{-23} m^{2}kg s^{-2}K^{-1}
Light speed (c)	$300,000$ km s^{-1}
SMAP's main-lobe antenna gain ($g_{(ml)}$)	0 dB
SMAP's side-lobe antenna gain ($g_{(sl)}$)	-60 dB
Central Carrier frequency of BS (f)	1.413 GHz
BS transmission bandwidth (β)	24 MHz
Earth radius (r_e)	6371 km
SMAP's distance to Earth's center (h)	7056 km
Min. possible distance to SMAP ($d_{\min}$)	$h - r_e = 685$ km
Max. possible distance to SMAP ($d_{\max}$)	$\sqrt{h^2 - r_e^2} = 3032.7$ km
Main-lobe distance to SMAP ($d_{(ml)}$)	865.5 km

Corollary 5. *The variance of $T_{(ml)}$ defined in* (18) *is:*

$$Var[T_{(sl)}] = \frac{2\pi}{2-2\alpha}\left(\frac{r_e}{h}\right) g_{(sl)}^2 \eta^2 \omega^{2\alpha} \lambda_c (\lambda_{BS}^2 + \lambda_{BS}) \left(d_{max}^{2-2\alpha} - d_{min}^{2-2\alpha}\right). \tag{28}$$

Proof. Based on Remark 1, the variance of $T_{(sl)}$ is its second cumulant defined in (26). □

IV. Numerical Results

In this section, we evaluate the RFI brightness temperature statistics at both SMAP's main- and side-lobes based on the analysis in the previous sections. The simulation parameters are given in Table I. Based on this table, an average of one cluster exists in every 10000 km^2 and, on average, 2500 BS clusters exist in the area exposed to the satellite. We also set SMAP's side-lobe gain to a conservative -60 dB. We allocate a transmission bandwidth of 24 MHz to each BS, complemented by a 3 MHz guard-band, resulting in a total of 27 MHz within the restricted L-band spectrum.

Due to space limitations, we only assess the average and standard deviation (STD) of RFI brightness temperature at SMAP's main- and side-lobes. We use these metrics to determine if the values fall within an acceptable error range. Figure 4 illustrates the findings. In Figure 4a, the average RFI brightness temperature at SMAP's main-lobe far exceeds the acceptable threshold $\tau = 1.3K$, ranging from 200 to 800 Kelvin. Figure 4b shows a high STD in the range of hundreds, indicating extreme uncertainty in RFI. Notably, 7 to 28 base stations, on average, contribute to these RFI characteristics.

Now we focus on RFI brightness temperature on SMAP's side-lobe depicted in Figures 4c and 4d. As observable in figure 4c, for clusters with an average of 50 and 100 active BSs, the average RFI brightness temperature falls within the acceptable threshold of $1.3K$, while for clusters of average 200 active BSs, the average RFI brightness temperature slightly exceeds the limit. Also, from Figure 4d, we see extremely low STD values for RFI brightness on SMAP's side-lobe, which is an indicator of extremely low uncertainty in RFI.

V. Conclusion

In this paper, we introduced an innovative method using cluster processes in stochastic geometry to evaluate RFI brightness temperature on passive remote sensing satellites. Our model is tailored to NASA's SMAP satellite, passively operating in the restricted L-band 1400 to 1427 MHz. Interestingly, our findings show that, while avoiding active base stations in main-lobe antenna footprint through satellite positioning, SMAP's antenna's remarkably low side-lobe gains allow for numerous active co-channel cellular base stations without compromising measurement precision.

Appendix A
Proof to Lemma 3

Since SMAP's main-lobe antenna footprint is roughly 40^2 km^2, we note that $\Lambda = 40^2\lambda_c$. Thus, conditioned on M we note that:

$$M_{(ml)}(t) = \mathbb{E}_M\left[\mathbb{E}\left[\exp\left(t\sum\nolimits_M T_{cluster}(\mathtt{x})\right)\right]\right]. \tag{29}$$

The inner $\mathbb{E}[\cdot]$ is the MGF of the sum of M clusters defined in (12), and based on (13), can be expressed as:

$$\mathbb{E}\left[\exp\left(t\sum\nolimits_m T_{cluster}(\mathtt{x})\right)\right] = \left(M_{cluster}(t;\, d_{(ml)},\, g_{(ml)})\right)^m. \tag{30}$$

Accordingly, (29) can be expanded as:

$$M_{(ml)}(t) = \sum_{m=0}^{\infty} \frac{e^{-\Lambda}\Lambda^m}{m!}\left(M_{cluster}(t;\, d_{(ml)},\, g_{(ml)})\right)^m, \tag{31}$$

which is equivalent to (20).

Appendix B
Proof to Lemma 4

For ease of notation, in (21) we define $T_{\mathbf{X}_i} := T_{cluster}(\mathbf{X}_i)$. Accordingly, the MGF of (21) is as:

$$M_{(sl)}(t) = \mathbb{E}\left[e^{tT_{(sl)}}\right] = \mathbb{E}_{\Psi,\{T_{\mathbf{X}_i}\}}\left[\prod\nolimits_{\mathbf{X}_i\in\Psi^{(sl)}} e^{tT_{\mathbf{X}_i}}\right]. \tag{32}$$

Due to the initial assumption of the independence of clusters, we move the expectation with respect to $\{T_{\mathbf{X}_i}\}$ inside the product as:

$$\mathbb{E}_{\Psi_{(sl)}}\left[\prod\nolimits_{\mathbf{X}_i\in\Psi_{(sl)}} \mathbb{E}\left[e^{tT_{\mathbf{X}_i}}\right]\right], \tag{33}$$

which is the *Probability Generating Functional* (PGFL) [7] of $g(\mathtt{x}) = \mathbb{E}\left[e^{tT_{\mathtt{x}}}\right]$ over the set $\mathcal{B}_{(sl)}$ and can be written as:

$$\mathcal{P}_{\Psi_{(sl)}}(g) = \mathbb{E}_{\Psi_{(sl)}}\left[\prod_{\mathrm{X}_i\in\Psi_{(sl)}} g(\mathrm{X}_i)\right] = \exp\left(-\int_{\mathcal{B}_{(sl)}} (1-g(\mathtt{x}))\,\Lambda(d\mathtt{x})\right), \tag{34}$$

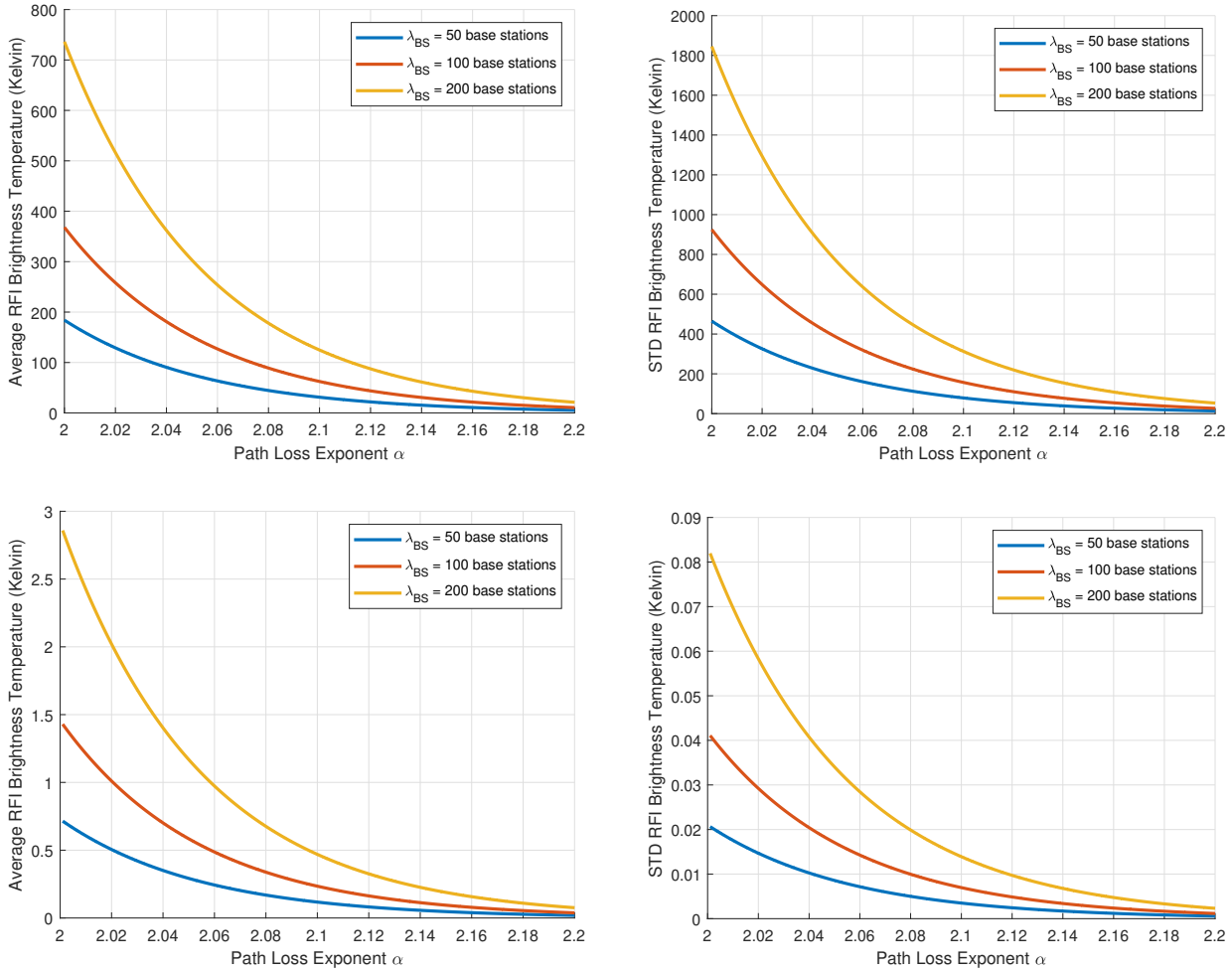

(c) Side-lobe average RFI brightness temperature.

(d) Side-lobe STD of RFI brightness temperature.

Figure 4: Average and Standard Deviation of RFI brightness temperature on SMAP's main- and side-lobes for average $\lambda_{BS} = 50,\ 100,\ 200$ active BSs in a cluster. On average $125,\ 250$ and 500 thousand base stations are exposed to SMAP's side-lobe, while only, on average, $7,\ 14$ and 28 base stations are exposed to SMAP's main-lobe.

where, based on Fig. (3), in spherical coordinates for equidistant points to SMAP for a PPP with intensity λ_c:

$$\Lambda\left(d\mathtt{x}\right) = 2\pi r^2 \lambda_c \sin(\theta)\, d\theta. \tag{35}$$

We note that $g(\mathtt{x})$ is the MGF of RFI brightness temperature of a cluster at point $\mathtt{x} \in \mathcal{B}_{(sl)}$ as in (13), which we note here with $g(\mathtt{x}) = M_{cluster}(t;\ \|\mathtt{x}-\mathtt{h}\|,\ g_{(sl)})$, where $x = \|\mathtt{x}-\mathtt{h}\|$ is the distance to SMAP. From Fig. (3), and using the law of cosines, we note that:

$$x = \left(r_e^2 + h^2 - 2hr_e\cos(\theta)\right)^{\frac{1}{2}}, \tag{36}$$

with:

$$\begin{aligned} dx &= hr_e \sin(\theta)\left(r_e^2 + h^2 - 2hr_e\cos(\theta)\right)^{-\frac{1}{2}}\ d\theta \\ \Rightarrow x\ dx &= hr_e\sin(\theta)\ d\theta. \end{aligned} \tag{37}$$

Comparing (35) and (37), we note that:

$$\Lambda\left(d\mathtt{x}\right) = 2\pi\left(\frac{r_e}{h}\right)\lambda_c x\ dx, \tag{38}$$

where x is in the range of d_{max} and d_{min}. By substituting (38) in (34), we will have (22).

References

[1] e. a. Polese, Michele, "Coexistence and spectrum sharing above 100 ghz," *Proceedings of the IEEE*, 2023.

[2] e. a. Zheleva, Mariya, "Radio dynamic zones: Motivations, challenges, and opportunities to catalyze spectrum coexistence," *IEEE Commun. Mag.*, 2023.

[3] M. Afshang, H. S. Dhillon, and P. H. J. Chong, "Modeling and performance analysis of clustered device-to-device networks," *IEEE Trans. Wireless Commun.*, vol. 15, no. 7, pp. 4957–4972, 2016.

[4] D. Entekhabi et al., "SMAP handbook–soil moisture active passive: Mapping soil moisture and freeze/thaw from space," 2014.

[5] C. S. Turner, "Johnson-nyquist noise," *url: http://www. claysturner. com/dsp/Johnson-NyquistNoise*, 2012.

[6] K.-W. Hwang, C. S. Ryoo, and N. S. Jung, "Differential equations arising from the generating function of the (r, β)-bell polynomials and distribution of zeros of equations," *Mathematics*, vol. 7, no. 8, p. 736, 2019.

[7] F. Baccelli and B. Błaszczyszyn, "Stochastic geometry and wireless networks: Volume i theory," *Foundations and Trends® in Networking*, vol. 3, no. 3–4, pp. 249–449, 2010.